Cp), 1.8-2.0 (m, 4 H, CH_2), 1.2-1.5 (m, 4 H, CH_2), 0.75 ppm (d of m, 2 H, $^3J_{HF}$ = 12.9 Hz); ^{13}C NMR (75 MHz, C_6D_6, δ) 216.45, 216.41 (M-CO), 99.5 (d, $^1J_{CF}$ = 150.0 Hz, CF), 85.9 (Cp), 23.3 (d, $^2J_{CF}$ = 12.0 Hz, CH), 22.66 (CH_2), 19.52 ppm (d, $^3J_{CF}$ = 7.2 Hz, CH_2); ^{19}F NMR (282 MHz, C_6D_6, δ) -144.6 ppm (t, $^3J_{HF}$ = 12.7 Hz); mass spectrum *m/e* 290 (M^+), 271 (-F), 262 (-CO), 242 (-CO, -HF), 234 (-2CO), 214 (-2CO, -HF), 140 ($FeCpF^+$), 121 ($FeCp^+$); high-resolution calcd for $C_{14}H_{15}FFeO_2$ - 2CO 234.050 71, found 234.050 10, deviation -2.6 ppm. Elemental analysis could not be obtained since the compound is slowly decomposing.

Photolysis of Dicarbonyl(η⁵-cyclopentadienyl)(7-fluoro-7-bicyclo[4.1.0]heptyl)iron. A 0.015-g (0.05 mmol) sample of norcaryl σ complex **23** in 0.6 mL of benzene-d_6 was photolyzed in the ice bath for 6 h. No changes were observed in the ^1H NMR spectrum.

Synthesis of Dicarbonyl(η⁵-cyclopentadienyl)(η²-1,3-dimethylallene)iron Tetrafluoroborate (21). To a stirred solution of 0.200 g (0.76 mmol) of σ complex **17** in 10 mL of diethyl ether at 0 °C was added 0.094 mL (0.76 mmol, 0.108 g) of freshly distilled BF_3OEt_2 via steel cannula under nitrogen. A yellow solid precipitated immediately. The solvent was evaporated, and the solid was recrystallized from methylene chloride/diethyl ether to give 0.221 g (87%) of a 1:2.4 equilibrium mixture of syn and anti isomers. Spectral data are in agreement with the compound described in the literature:[2,7] mp 156-159 °C dec.; ^1H NMR (300 MHz, CD_2Cl_2, δ) major (anti-3-methyl) isomer 6.2 (m, 1 H), 5.7 (s, 5 H, Cp), 4.4 (m, 1 H), 2.1 (d of d, 3 H), 1.65 ppm (d, 3 H); ^1H NMR (300 MHz, CD_2Cl_2, δ) minor (syn-3-methyl) isomer 6.7 (m, 1 H), 5.7 (s, 5 H, Cp), 4.3 (m, 1 H), 2.2 (d of d, 3 H), 1.6 ppm (d, 3 H).

Synthesis of Dicarbonyl(η⁵-cyclopentadienyl)(η²-1,2-cycloheptadiene)iron Tetrafluoroborate (24). To a solution of 0.017 g (0.059 mmol) of norcaryl σ complex **23** in 10 mL of diethyl ether at 0 °C was added 7.27 μL (0.059 mmol) of freshly distilled BF_3OEt_2. A yellow precipitate appeared immediately. After the solvent was evaporated, a quantitative yield of a yellow solid was obtained. The product can be further purified by recrystallization from methylene chloride/diethyl ether. The compound has the same properties as **24** described in the literature:[9a] mp 145-148 °C dec.; ^1H NMR (300 MHz, CD_3NO_2, -20 °C, δ) 6.6 (m, 1 H, =C—H, free), 5.75 (s, 5 H, Cp), 4.3 (m, 1 H, =C-, complexed), 2.55 (m, 1 H), 2.35 (m, 2 H), 1.95 (m, 3 H), 1.6 (m, 1 H), 0.95 ppm (m, 1 H); ^{13}C NMR (75 MHz, CD_3NO_2, -20 °C, δ) 210.4, 207.4 (Fe—CO), 150.1 (=C=), 126.2 (-C=, free), 92.5 (Cp), 43.9 (-C=, complexed), 30.9, 30.8, 29.9, 29.5 ppm (CH_2).

Acknowledgment. This work was supported by the National Science Foundation to whom we are most grateful. Assistance of Otto Phanstiel during the early stages of this work is also acknowledged with appreciation.

Effect of Allyl Methyl Substituents on the Preparation, Dynamics, and Reactivity of $(\eta^5\text{-}C_5Me_5)(allyl)ZrX_2$ Complexes (X = Cl, Br): Structure of $(\eta^5\text{-}C_5Me_5)(C_3H_5)ZrCl_2$ and $(\eta^5\text{-}C_5Me_5)(1,2\text{-}Me_2(butadiene))(\eta^2\text{-}CH_2PPh_2)Zr$. Dynamics of $(\eta^5\text{-}C_5Me_5)(2,3\text{-}Me_2(butadiene))(\eta^2\text{-}CH_2PPh_2)Zr$

Peter J. Vance, Thomas J. Prins, Bryan E. Hauger, Michael E. Silver,* Michael E. Wemple, Lori M. Pederson, David A. Kort, Michael R. Kannisto, Steven J. Geerligs, Richard S. Kelly, and Jill J. McCandless

Department of Chemistry, Hope College, Holland, Michigan 49423

John C. Huffman and Dennis G. Peters

Department of Chemistry, Indiana University, Bloomington, Indiana 47405

Received July 19, 1990

This paper deals with the effects of methyl substituents on the allyl ligand on the preparation, dynamics, and reactivity of compounds of the type Cp*(allyl)ZrX_2 (**1**: allyl = C_3H_5, X = Cl; **3**: allyl = 1,1,2-trimethylallyl, X = Br; **4**: allyl = 1,2,3-trimethylallyl, X = Br). Methyl substituents on the allyl ligand at the terminal positions leads to increased yields of these compounds via the reaction of allyl Grignards or allyl lithium with Cp^*ZrCl_3. Cyclic voltammetry reveals that **3** and **4** are more difficult to reduce than Cp_2ZrX_2 (X = Cl, Br). Nevertheless, compounds **3** and **4** are reduced by $K[CpM(CO)_2]$ (M = Fe, Ru) yielding $[MCp(CO)_2]_2$ and uncharacterizable oils instead of bimetallic compounds. The reaction of **3** and **4** with 2 equiv of $LiCH_2PPh_2$ gives $Cp^*(\eta^4\text{-}2,3\text{-}Me_2(butadiene))(\eta^2\text{-}CH_2PPh_2)Zr$ (**5**) and $Cp^*(\eta^4\text{-}1,2\text{-}Me_2(butadiene))(\eta^2\text{-}CH_2PPh_2)Zr$ (**6**). X-ray crystallography of **6** reveals that the CH_2PPh_2 is bound through both the P and C atoms (Zr-C, 2.346 (8) Å; Zr-P, 2.664 (2) Å) to yield a highly strained Zr-C-P ring. For **6**: cell constants a = 12.386 (5) Å, b = 12.778 (6) Å, c = 9.223 (4) Å, α = 109.26 (2)°, β = 91.52 (2)°, γ = 109.66 (2)°; space group $P\bar{1}$; R = 0.0626, R_w = 0.0607. Variable-temperature ^1H NMR studies of **5** revealed a dynamic process involving Zr-P bond rupture ($\Delta G^\ddagger$ = 38.9 ± 1.0 kJ/mol). Also isolated in small amounts were crystals of **1** suitable for an X-ray structure determination, which revealed a prone orientation for the $\eta^3\text{-}C_3H_5$ allyl ligand. For **1**: cell constants a = 9.726 (2) Å, b = 11.214 (2) Å, c = 13.262 (3) Å; space group *Pnam*; R = 0.0367, R_w = 0.0401. The ^1H NMR spectrum of **4** has revealed the presence of a second isomer in which one of the terminal allyl methyls assumes an anti orientation (the major isomer has both terminal methyls in the syn orientation). A variable-temperature ^1H NMR study of **4** revealed an $\eta^3\text{-}\eta^1$-allyl isomerization mechanism that leads to exchange between isomers ($\Delta G^\ddagger$ = 66.2 ± 1.0 kJ/mol).

Introduction

In an earlier paper we presented the preparation and the first structural and dynamic studies of compounds of the type $Cp^*(\eta^3\text{-allyl})ZrBr_2$ ($Cp^* = C_5Me_5$; allyl = 1,1,2-trimethyl (**3**) or 1,2,3-trimethyl (**4**)).[1] These complexes can be thought of as zirconocene dihalide analogues in which one Cp has been replaced with an allyl ligand. The

(1) Larson, E. J.; Van Dort, P. C.; Dailey, J. S.; Lakanan, J. R.; Pederson, L. M.; Silver, M. E.; Huffman, J. C.; Russo, S. O. *Organometallics* 1987, *6*, 2141.

0276-7333/91/2310-0917$02.50/0

reactivity of zirconocene dihalides such as Cp_2ZrCl_2 has been exhaustively studied over the years.[2] The effect of permethylating the Cp rings to yield $Cp^*_2ZrCl_2$ has led to further interesting reactivity not known for the unmethylated analogues.[3] To this date much less has been done to determine the effect of allyl methyl substituents on the preparation and reactivity of early-transition-metal allyl complexes. The reactivity of $Cp^*(\eta^3\text{-allyl})ZrX_2$ compounds should be very different from metallocene analogues, since the η^3-allyl ligand supplies two fewer electrons to the metal than Cp and it often undergoes rapid η^3–η^1 isomerization.[1,4-6] In addition, complexed allyl ligands that are methylated at the terminal positions can undergo proton abstraction to yield butadiene complexes.[7,8] We report here on the effect of allyl methyl substituents on the preparation of $Cp^*(\eta^3\text{-allyl})ZrX_2$ compounds and on their reactivity with late-transition-metal anions $[MCp(CO)_2]^-$ (M = Fe, Ru) and with $LiCH_2PPh_2$. We also report on the structures of the new compounds $Cp^*(C_3H_5)ZrCl_2$ (1) and $Cp^*(1,2\text{-}Me_2(\text{butadiene}))(\eta^2\text{-}CH_2PPh_2)Zr$ (6), the first structurally characterized example of a Zr complex η^2-bound to a CH_2PPh_2 ligand. Finally, we report on the dynamics and isomers of $Cp^*(1,2,3\text{-}Me_3(\text{allyl}))ZrBr_2$ (4), and the dynamics of $Cp^*(2,3\text{-}Me_2(\text{butadiene}))(\eta^2\text{-}CH_2PPh_2)Zr$ (5).

Experimental Section

General Comments. Ether, THF, and hexane were distilled from sodium/benzophenone under argon. THF solutions of LiC_3H_5 were prepared by the method of Seyferth and Weiner.[9] $Cp^*(1,1,2\text{-}Me_3C_3H_2)ZrBr_2$ (3) and $Cp^*(1,2,3\text{-}Me_3C_3H_2)ZrBr_2$ (4) were prepared as described previously [the only modification was that both (1,1,2-Me_3(allyl))MgBr and (1,2,3-Me_3(allyl))MgBr were prepared in diethyl ether].[1] Cp^*ZrCl_3 was prepared and used in situ (isolation did not improve subsequent yields).[10] $LiCH_2PPh_2$ was prepared as described elsewhere.[22] Zirconium tetrachloride and THF solutions of $BrMg(C_3H_5)$ (titrated via the method of Eastham and Watson[12]) were purchased from the Aldrich Chemical Co. and used without further purification. All syntheses and subsequent handling of compounds were conducted under anhydrous conditions in a dry argon atmosphere. Elemental analyses were performed by Dornis and Kolbe Mikroanalytisches Laboratorium, West Germany.

$Cp^*Zr(C_3H_5)Cl_2$ (1). An ether solution of lithium allyl (0.260 M, 33.0 mL, 8.58 mmol) was added dropwise over 1 h to a stirred solution of Cp^*ZrCl_3 prepared in situ (LiCp* 1.21 g, 8.58 mmol; $ZrCl_4$ 2.00 g, 8.58 mmol; 100 mL of diethyl ether). The reaction solution was then reduced in volume to ~75 mL via trap to trap distillation, causing LiCl and tetraphenyltin (present in the lithium allyl solution) to precipitate. The reaction solution was filtered to yield an orange filtrate. Successive precipitations at −40 °C yielded 0.52 g of product (yellow powder) contaminated with tetraphenyltin. This material was used for NMR studies. Recrystallization from diethyl ether yielded suitable yellow rectangular crystals for an X-ray structure determination. ^{1}H NMR ($CDCl_3$/TMS 2%): δ 5.97 (p, CH, allyl, 1 H), 3.42 (d, CH_2, allyl, 4 H), 2.08 (CH_3, Cp*, 15 H). ^{1}H NMR (toluene-d_8/TMS 2%): δ 5.37 (p, CH, allyl, 1 H), 3.13 (d, CH_2, allyl, 4 H), 1.73 (CH_3, Cp*, 15 H).

$Cp^*Zr(C_3H_5)Br_2$ (2). To a stirred solution of Cp^*ZrCl_3 prepared in situ (HCp* 1.315 g, 9.64 mmol; *n*-BuLi 9.64 mmol; $ZrCl_4$ 2.26 g, 9.70 mmol; 150 mL of ether) was rapidly added an ether solution of allyl magnesium bromide (0.966 M, 10.0 mL, 9.66 mmol). The reaction apparatus was then immediately cooled via a dry ice/2-propanol bath to −78 °C. From this point on, all solutions and isolated solids were never allowed to warm above −78 °C until isolation of final product. The reaction solution was stirred for 1 h, during which time the color changed from pale yellow to deep red. The solution was then filtered, yielding a deep red filtrate. The filtrate was reduced in volume to ~80 mL via trap to trap distillation and cooled to −88 °C via a refrigerated methanol bath for 2 days to yield an orange powder. The orange powder was isolated via cannula, and the solution was transferred to a receiving flask. The orange powder, a combination of magnesium halide salts and product, was washed successively with two 5-mL portions of hexane. These washes were combined with the previously isolated solution via cannula. The remaining orange powder was discarded. The volume of the red solution was then reduced to ~45 mL by trap to trap distillation and then cooled to −88 °C to yield an orange precipitate. The orange precipitate was isolated from the red solution via cannula and vacuum dried. Further workup of the red solution yielded no significant amount of product. The orange precipitate was dissolved with 30 mL of ether, yielding an orange solution and insoluble white magnesium salts. The orange solution was isolated via filtration and reduced in volume to ~5 mL via trap to trap distillation. Orange crystals (0.040 g, 0.96%) were produced upon cooling to −88 °C and were isolated and pumped dry. NMR analysis indicated that the product was slightly contaminated with solvated (diethyl ether) magnesium salts. ^{1}H NMR ($CDCl_3$/TMS 2%): δ 5.82 (p, CH, allyl, 1 H), 3.53 (d, CH_2, allyl, 4 H), 2.12 (CH_3, Cp*, 15 H). A variable-temperature ^{1}H NMR study ($CDCl_3$/TMS 2%) yielded a $\Delta G^\ddagger = 54.9 \pm 1.0$ kJ/mol for η^3–η^1 isomerization, obtained from equilibration of the signals due to syn and anti protons (coalescence at −6.0 °C).

$Cp^*(2,3\text{-}Me_2(\text{butadiene}))(CH_2PPh_2)Zr$ (5). Approximately 40 mL of ether were added to a mixture of 0.800 g (1.7 mmol) of 3 and 0.703 g (3.4 mmol) of $LiCH_2PPh_2$. The resulting slurry was stirred. The reaction solution turned a clear dark red within 5 min and remained so throughout the reaction. After 1 h, the solvent was removed via trap to trap distillation. The remaining solid was extracted with 60 mL of hexane and filtered. Successive crystallizations at −40 °C from the filtrate yielded 0.205 g (23.7%) of pale red powder. Anal. Calcd for $C_{29}H_{37}ZrP$: C, 68.59; H, 7.34; Zr, 17.96; P, 6.10. Found: C, 68.49; H, 7.46; Zr, 17.84; P, 6.04. ^{1}H NMR: (toluene-d_8/TMS 2%) δ 7.52 (m) and 6.97 (m) (CH, phenyl, 10 H), 1.88 (CH_3, Cp*, 15 H), 1.85 (CH_3, butadiene, 6 H),

(2) Cardin, D. J.; Lappert, M. F.; Raston, C. L. *Chemistry of Organo-Zirconium and -Hafnium Compounds*; John Wiley & Sons: New York, 1986.

(3) Manriquez, J. M.; McAlister, D. R.; Rosenberg, E.; Shiller, A. M.; Williamson, K. L.; Chan, S. I.; Bercaw, J. E. *J. Am. Chem. Soc.* **1978**, *100*, 3078.

(4) Larson, E. J.; Van Dort, P. C.; Lakanen, J. R. O'Neil, D. W.; Pederson, L. M.; McCandless, J. J.; Silver, M. E.; Russo, S. O.; Huffman, J. C. *Organometallics* **1988**, *7*, 1183.

(5) (a) Faller, J. W. *Adv. Organomet. Chem.* **1977**, *16*, 211. (b) Tsutusi, M.; Courtney, A. *Ibid.* **1977**, *16*, 241.

(6) Faller, J. W.; Thomsen, M. E.; Mattina, M. J. *J. Am. Chem. Soc.* **1971**, *93*, 2642.

(7) Hessen, B.; Spek, A. L.; Teuben, J. H. *Angew. Chem., Int. Ed. Engl.* **1988**, *8*, 1058.

(8) Berg, K.; Erker, G. *J. Organomet. Chem.* **1984**, *270*, C53.

(9) Seyferth, D.; Weiner, W. A. *J. Org. Chem.* **1961**, *26*, 4797.

(10) Wengrivius, J. H.; Schrock, R. R. *J. Organomet. Chem.* **1981**, *205*, 319.

(11) Schore, N. E.; LaBelle, B. E. *J. Org. Chem.* **1981**, *46*, 2306.

(12) Watson, S. C.; Eastham, J. F. *J. Organomet. Chem.* **1967**, *9*, 165.

(13) Ibers, J. A.; Hamilton, W. C., Eds. *International Tables for X-Ray Crystallography*; Kynoch: Birmingham, England, 1974; Vol. 4.

(14) Huffman, J. C.; Lewis, L. N.; Caulton, K. G. *Inorg. Chem.* **1980**, *19*, 2755.

(15) Erker, G.; Berg, K.; Angermund, K.; Kruger, C. *Organometallics* **1987**, *6*, 2620.

(16) Blenkers, J.; De Liefde Meijer, H. J.; Teuben, J. H. *J. Organomet. Chem.* **1981**, *218*, 383.

(17) Blenkers, J.; Hessen, B.; Bolhuis, F.; Wagner, A. J.; Teuben, J. H. *Organometallics* **1987**, *6*, 459.

(18) ^{1}H NMR NMR spectral simulations were carried out by using the program PCPMR, which can accommodate eight $I = {}^1/_2$ nucleii simultaneously. The program was obtained from Serena Software Inc., P.O. Box 3076, Bloomington, IN 47402.

(19) Casey, C. P.; Jordan, R. F. *Organometallics* **1984**, *3*, 504.

(20) Schore, N. E.; Hope, H. *J. Am. Chem. Soc.* **1980**, *102*, 4251.

(21) Choukroun, R.; Iraqi, A.; Gervais, D.; Daran, J. C.; Jeannin, Y. *Organometallics* **1987**, *6*, 1197.

(22) Sartain, W. J.; Selegue, J. P. *Organometallics* **1987**, *6*, 1812.

1.58 (Br d, CH, butadiene, exo, 2 H), 0.45 (d, P–CH_2, 2 H), 0.23 (br t, CH, butadiene, endo, 2 H). ^{1}H NMR (THF-d_8/TMS 2%) 7.58 (m) and 7.23 (m) (CH, phenyl, 10 H), 1.84 (CH_3, Cp*, 15 H), 1.64 (CH_3, butadiene, 6 H), 1.22 (br d, CH, butadiene, exo, 2 H), 0.34 (d, P–CH_2, 2 H), –0.10 (br t, CH, butadiene, endo, 2 H).

Cp*(1,2-Me_2(butadiene))(CH_2PPh_2)Zr (6). Approximately 40 mL of ether were added to a mixture of 0.294 g (0.63 mmol) of 4 and 0.258 g (1.3 mmol) of $LiCH_2PPh_2$. The resulting slurry was stirred. The reaction solution turned a clear dark red-brown within 5 min and remained so throughout the reaction. After 70 min, the solvent was removed via trap to trap distillation and the solid residue was extracted with 35 mL of hexane and filtered. The filtrate was reduced in volume to 10 mL. Cooling to –40 °C yielded 0.150 g (47.2%) of dark, red-brown crystalline solid. Anal. Calcd for $C_{29}H_{37}ZrP$: C, 68.59; H, 7.34; Zr, 17.96; P, 6.10. Found: C, 68.50; H, 7.42; Zr, 17.88; P, 6.02. ^{1}H NMR (toluene-d_8): δ 7.70 (m), 7.46 (m), and 6.97 (m) (CH, phenyl, 10 H); 5.84 (br m, CH, butadiene, 1 H); 1.91 (CH_3, Cp* and CH, butadiene, exo, 16 H); 1.54 (CH_3, butadiene, 3 H); 1.42 (d, CH_3, butadiene, 3 H); 0.44 (d, P–CH, 1 H); 0.40 (d, P–CH, 1 H); 0.02 (m, CH, butadiene, endo on unmethylated C, 1 H) –0.08 (br m, CH, butadiene, endo on methylated C, 1 H).

Nuclear Magnetic Resonance Spectra. Proton chemical shifts were measured with a General Electric OMEGA GN-300 300 MHz spectrometer. Peak positions are reported as δ in parts per million relative to TMS at δ 0 in THF-d_8 or relative to Dow Corning high-vacuum silicone grease at δ 0.26 in toluene-d_8. Temperatures, determined by a copper/constantan thermocouple in the probe assembly, are estimated to be accurate to ±1.0 °C. Peak assignments for the ambient-temperature spectra of compounds 4 and 6 were accomplished via the 2D-COSY technique.

Electrochemical Measurements. Electrochemical measurements were carried out under argon inside a Vacuum Atmospheres drybox. Techniques employed were cyclic voltammetry (CV) and linear scan voltammetry (LSV) at a rotating-disk electrode (RDE).

Potentials are referred to a silver/silver chloride electrode containing a fill solution of 0.1 M tetra-*n*-butylammonium perchlorate in THF that was saturated with silver nitrate. The potential of this electrode was +0.65 V versus the saturated calomel electrode. The supporting electrolyte was tetra-*n*-butylammonium hexafluorophosphate (Aldrich) for Cp_2ZrX_2 (X = Cl, Br) or tetra-*n*-butylammonium perchlorate (GFS Chemicals) for compounds 3 and 4 at a concentration of 0.1 M. Both supporting electrolyes were recrystallized twice from ethanol/water and vacuum dried at 100 °C.

An IBM Instruments Model EC/225 voltammetric analyzer was employed as the potentiostat, with the voltammetric curves being recorded on a Hewlett-Packard Model 7030AM X-Y recorder. All experiments employed a conventional three-electrode configuration with a platinum wire auxiliary electrode. The working electrodes were 2 mm diameter platinum disks sealed in Kel-F (Bioanalytical Systems, Inc.). Electrodes were polished with slurries of 1, 0.3, and 0.05 μm aluminum micropolish on microcloth pads (all Buehler Ltd.) and cleaned by sonication in distilled water before use.

For rotating-disk electrode measurements, an Eberbach synchronous rotator (VWR Scientific) was employed at 1000 rpm. The resulting plateau currents were compared to known one-electron standards (cobaltocenium hexafluorophosphate and ferrocene, both from Aldrich and used as received) to estimate *n* values for the compounds measured. All gave *n* values close to one.

All electrochemical glassware was cleaned by soaking in an alcoholic KOH bath, followed by treatment with dilute acid. Glassware was then dried at 110 °C and introduced into the evacuation chamber of the drybox while still hot to avoid adsorption of water. Once inside the drybox, all glassware and electrodes were rinsed several times with the electrochemical solvent prior to use. Tetrahydrofuran was employed as the electrochemical solvent for all measurements.

X-ray Structural Determinations. Pertinent data for the structures of compounds 1 and 6 are in Table I. The crystals were mounted on a computer-controlled Picker four-circle diffractometer equipped with a Furnas monochromator (HOG crystal) and cooled by a gaseous nitrogen cooling system. A

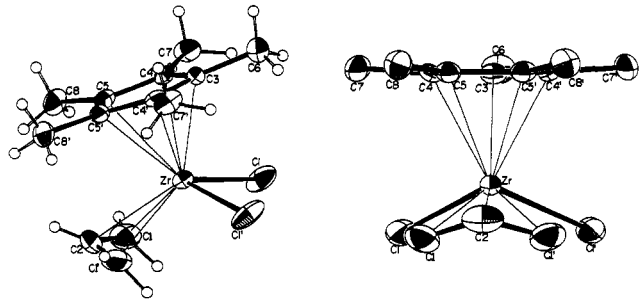

Figure 1. ORTEP diagrams of Cp*(C_3H_5)$ZrCl_2$ (1). The left view emphasizes the bent-metallocene type geometry. The right view shows the pseudotetrahedral geometry and the prone orientation of the allyl ligand with respect to Cp*.

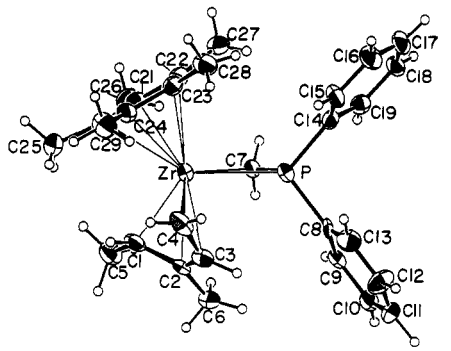

Figure 2. ORTEP diagram of Cp*(1,2-$Me_2C_4H_4$)(CH_2PPh_2)Zr (6). The Cp* ring atom C20 is obscured.

systematic search of a limited hemisphere of reciprocal space for 1 located a set of diffraction maxima with systematic absences consistent with the orthorhombic space group *Pnam* (*Pnam* is an alternate setting of *Pnma*). A similar search for 6 revealed no symmetry or systematic absences, indicating a triclinic space group. Subsequent solution and refinement of the structure confirmed the centrosymmetric choice $P\bar{1}$. Orientation matrices and accurate unit cell dimensions were determined at low temperature from least-squares fits of 32 reflections ($20° < 2\theta < 30°$) for both 1 and 6. Intensity data were collected by using the $\theta/2\theta$ scan method; four standard reflections, monitored every 300 reflection measurements, showed only statistical fluctuations for both compounds. No absorption correction was performed for either compound due to their small and roughly equal dimensions and the small value of their linear absorption coefficients. Both structures were refined successfully without this correction. The intensities were corrected for Lorentz and polarization factors and scaled to give the numbers of independent F_{hkl} values for $I > 2.33\sigma(I)$ indicated in Table I.

Both structures were solved by a combination of direct methods (MULTAN78) and Fourier techniques. All atoms, including hydrogens, were located for both compounds. For both compounds, all non-hydrogen atoms were refined anisotropically and all hydrogen atoms were refined isotropically; refinements converged to values for the conventional *R* indices shown in Table I. The maximum residuals in the final difference Fourier synthesis for 1 and 6 were 0.56 and 0.39 e/Å^3, respectively. The weighting scheme used in the final calculations was of the form $w = 1/\sigma_F^2$. Scattering factors were taken from ref 13. The scattering factor for the Zr and Cl atoms were corrected for the real and imaginary parts of anomalous dispersion by using values from ref 13. All computations were carried out on a 386 PC using programs described elsewhere.[14] The positional parameters and equivalent isotropic thermal parameters for the non-hydrogen atoms are listed in Table II, the atom-numbering schemes being shown in Figures 1 and 2 for compounds 1 and 6, respectively. Anisotropic thermal parameters for the non-hydrogen atoms are listed in Table III (supplementary material), hydrogen atom coordinates and isotropic thermal parameters in Table IV (supplementary material), and structure factors in Tables V and VI (supplementary material) for compounds 1 and 6, respectively.

Table I. Summary of Crystal Data and Intensity Collection for $Cp^*(C_3H_5)ZrCl_2$ (1) and for $Cp^*(1,2\text{-}Me_2C_4H_4)(CH_2PPh_2)Zr$ (6)

	1	6
formula	$C_{13}H_{20}ZrCl_2$	$C_{29}H_{37}ZrP$
fw	338.43	507.81
a, Å	9.726 (2)	12.386 (5)
b, Å	11.241 (2)	12.778 (6)
c, Å	13.262 (3)	9.223 (4)
α, deg	90.0	109.26 (2)
β, deg	90.0	91.52 (2)
γ, deg	90.0	109.66 (2)
V, Å^3	1450.04	1281.90
Z	4	2
d, g cm^{-3}	1.550	1.316
space group	*Pnam*	$P\bar{1}$
cryst dimens, mm	0.25 × 0.25 × 0.25	0.25 × 0.20 × 0.20
temp, °C	-155	-155
λ(Mo Kα radiation), Å	0.710 69	0.710 69
linear abs coeff, cm^{-1}	10.925	4.955
receiving aperture, mm	3.0 × 4.0; 22.5 cm from crystal	3.0 × 4.0; 22.5 cm from crystal
take-off angle, deg	2.0	2.0
scan speed, deg min^{-1}	6.0 (in 2θ)	4.0 (in 2θ)
bkgd counts, s	6 (at each end)	6 (at each end)
2θ limits, deg	6–45	6–45
data collcd	*hkl*	h,±*k*,±*l*
no. of unique data	1007	3347
no. of unique data with $F_o^2 > 2.33\sigma(F_o^2)$	888	2811
$R(F)$	0.0367	0.0626
$R_w(F)$	0.0401	0.0607

Results and Discussion

Synthesis of $Cp^*(allyl)ZrX_2$ Compounds (allyl = $C_3Me_nH_{5-n}$, n = 0, 3; X = Cl, Br). We have prepared compounds of this type in ether by the dropwise addition of solutions of either an allyl Grignard or lithium allyl reagent to a stirred solution of an equivalent of Cp^*ZrCl_3.

$$Cp^*ZrCl_3 + Li(C_3H_5) \xrightarrow[Et_2O]{} \underset{\mathbf{1}}{Cp^*(\eta^3\text{-}C_3H_5)ZrCl_2} \quad (1)$$

$$Cp^*ZrCl_3 + BrMg(allyl) + MgBr_2\ (excess) \xrightarrow[Et_2O]{} \underset{\mathbf{2\text{-}4}}{Cp^*(\eta^3\text{-}allyl)ZrBr_2}$$

allyl = C_3H_5 (**2**), 1,1,2-$Me_3C_3H_2$ (**3**), 1,2,3-$Me_3C_3H_2$ (**4**)

These reactions are plagued by low yields which are invariant to reaction temperature (−78 °C to room temperature) or solvent (ether, THF, hexane). A number of observations suggest that this is most likely due to the kinetics of the substitution reactions involved and that the above reactions initially produce tris(allyl) complexes. An indication of this is that our reaction solutions take on an intense red or red-brown color within addition of 25% of the Grignard whereas products **1–4** are orange crystalline solids that yield orange solutions in ether. An intense red color has been associated with solutions of $CpZr(allyl)_3$ and $Cp^*Zr(allyl)_3$ compounds or their decomposition products.[15,16] For example, $Cp^*(1\text{-}MeC_3H_4)_3Zr$ is stable in solution up to −40 °C, whereupon it decomposes to give an intensely colored solution from which the red allyl–butadiene complex $Cp^*(1\text{-}Me(allyl))(C_4H_6)Zr$ is isolated.[16] Such butadiene–allyl complexes can then undergo ligand exchange with unreacted Cp^*ZrCl_3 to yield our $Cp^*Zr(allyl)X_2$ complexes.[17] If this were the only route to final product, the maximum yield would be 33%. It is of interest to note that our best yields for **3** and **4** are 24.2% and 33.8%, respectively.[1] However, tris(C_3H_5) complexes cannot decompose to give butadiene–allyl compounds.

Table II. Coordinates (×10^4) and Equivalent Isotropic Temperature Factors for $Cp^*(C_5H_5)ZrCl_2$[a] (1) and $Cp^*(1,2\text{-dimethyl-}1,3\text{-butadiene})(CH_2PPh_2)Zr$[a] (6)

	x	y	z	U, Å^2
		Compound 1		
Zr	8815 (1)	10454 (1)	7500*	1.5
Cl	8461 (2)	1866 (1)	6137 (1)	3.4
Cl′	8461 (2)	1866 (1)	8863 (1)	3.4
C1	10918 (7)	9981 (7)	6597 (6)	3.4
C1′	10918 (7)	9981 (7)	8403 (6)	3.4
C2	11079 (9)	9394 (9)	7500*	3.1
C3	6438 (7)	9761 (6)	7500*	1.5
C4	7041 (5)	9325 (4)	8363 (4)	1.5
C4′	7041 (5)	9235 (4)	6637 (4)	1.5
C5	8039 (5)	8396 (5)	8044 (4)	1.7
C5′	8039 (5)	8396 (5)	6956 (4)	1.7
C6	5258 (10)	10631 (9)	7500*	2.7
C7	6638 (7)	9458 (6)	9438 (5)	2.4
C7′	6638 (7)	9458 (6)	5562 (5)	2.4
C8	8827 (7)	7559 (6)	8705 (5)	2.5
C8′	8827 (7)	7559 (6)	6295 (5)	2.5
		Compound 6		
Zr	8378 (1)	6792 (1)	9113 (1)	1.8
P	6885 (2)	7882 (2)	10014 (2)	1.9
C1	10184 (7)	7318 (7)	10587 (9)	2.4
C2	9536 (6)	7737 (7)	11761 (8)	2.4
C3	8444 (7)	6979 (8)	11845 (9)	3.0
C4	7918 (7)	5769 (8)	10791 (10)	3.4
C5	11384 (7)	8130 (8)	10496 (10)	3.1
C6	9990 (7)	9032 (8)	12808 (9)	3.2
C7	8184 (6)	8613 (7)	9413 (8)	2.1
C8	6765 (6)	8720 (6)	12005 (8)	1.9
C9	7504 (6)	9856 (7)	12829 (9)	2.1
C10	7362 (7)	10428 (7)	14344 (9)	2.5
C11	6494 (7)	9860 (8)	15029 (9)	2.9
C12	5748 (8)	8722 (8)	14202 (10)	3.5
C13	5892 (7)	8154 (7)	12708 (10)	3.0
C14	5608 (6)	7841 (6)	8900 (8)	2.0
C15	4622 (7)	6805 (7)	8423 (10)	2.7
C16	3628 (7)	6775 (8)	7658 (10)	3.3
C17	3602 (7)	7750 (8)	7368 (10)	2.9
C18	4578 (6)	8776 (7)	7836 (9)	2.4
C19	5584 (6)	8829 (7)	8604 (8)	2.2
C20	9094 (6)	5564 (7)	6921 (9)	2.5
C21	8949 (6)	6479 (6)	6447 (8)	2.0
C22	7749 (7)	6265 (6)	6250 (9)	2.6
C23	7147 (7)	5236 (6)	6621 (8)	2.4
C24	7981 (6)	4796 (7)	7012 (9)	2.5
C25	10214 (8)	5363 (8)	7110 (10)	3.3
C26	9886 (7)	7458 (7)	6167 (9)	2.9
C27	7204 (7)	6934 (7)	5602 (9)	2.5
C28	5868 (7)	4637 (7)	6437 (10)	3.1
C29	7704 (8)	3677 (7)	7342 (11)	3.4

[a] Parameters marked by an asterisk were not varied. Estimated standard deviations are given in parentheses. Equivalent isotropic thermal parameters are calculated by using the formula given by: Hamilton, W. C. *Acta Crystallogr.* **1959**, *12*, 609.

Accordingly, our best yields for **1** and **2** were extremely low and we were unable to obtain satisfactory analyses due to contamination with either Ph_4Sn present in the lithium allyl solutions or etherated magnesium halide salts present in the Grignard solutions. Repeated microrecrystallizations yielded a few yellow-orange crystals of pure **1** that were suitable for X-ray structure determination. Even though satisfactory elemental analyses of **1** and **2** could not be obtained, their ^1H NMR spectra were consistent with the expected structure and could be reproduced by NMR simulation.[18] The NMR data for compounds **1** and **2** (along with a ΔG^* for η^3–η^1 isomerization in **2** obtained from a variable-temperature ^1H NMR study) are offered in the Experimental Section. It is of interest to note that the ΔG^* measured for **2** (54.9 ± 1.0 kJ/mol) is 3.4 kJ/mol greater than that for the analogous process in **3** (ΔG^* = 51.5 kJ/mol). This is expected since only in compound

Table VII. Cyclic Voltammetric Measurements versus Ag/AgCl

compd	position of first redn wave, V	$E°_{red}$, V
Cp_2ZrCl_2	-2.46	-2.36
Cp_2ZrBr_2	-2.24	2.17
3	-2.64	
4	-2.52	

3 is the η^3-allyl ligand significantly distorted towards an η^1 mode, lowering the barrier for its isomerization.[1]

Reactivity of Cp*(η^3-$Me_3C_3H_2$)$ZrBr_2$ Complexes. Earlier work of ours detailed the preparation, structure, and dynamic properties of **3** and **4**.[1] Our efforts since then have focused on the reactivity of these compounds. In particular we were interested in whether Cp*(allyl)ZrX_2 compounds could serve as precursors to early–late-transition-metal complexes as do zirconocene dihalides. For example, Cp_2ZrCl_2 reacts with K[CpM(CO)$_2$] (M = Fe, Ru) to form heterobimetallics with a direct metal-to-metal bond[19] or with 2 equiv of $LiCH_2PPh_2$ to yield $Cp_2Zr(CH_2PPh_2)_2$, which has been used to form bimetallics via chelation of late-transition metals at the P atoms.[20,21] We have found that slow addition of ether or THF solutions of **3** or **4** at room temperature to 1 equiv of K[CpM(CO)$_2$] (M = Fe, Ru) in THF gives near-quantitative yields of dimeric $[CpM(CO)_2]_2$ and KBr along with uncharacterizable dark oils.

$$\underset{\mathbf{3,\ 4}}{Cp^*(allyl)ZrBr_2} + K[MCp(CO)_2] \rightarrow [MCp(CO)_2]_2 + KBr + \text{uncharacterized oil}$$

allyl = 1,1,2-$Me_3C_3H_2$ (**3**), 1,2,3-$Me_3C_3H_2$ (**4**)

M = Fe, Ru

One possibility is that we are forming the desired heterobimetallics of the type Cp*(trimethylallyl)BrZr–MCp(CO)$_2$ but that the Zr–M bond suffers rapid homolytic cleavage, effectively reducing the Zr center. Such homolytic bond cleavage is observed for $(NMe_2)_3Ti$–FeCp(CO)$_2$, which decomposes rapidly at room temperature to give $[FeCp(CO_2)]_2$ and intractable titanium products.[22] When we follow our reactions by ^{1}H NMR spectroscopy in THF-d_8, we observe that **3** reacts instantaneously with the late-transition-metal anion to give a late-transition-metal dimer. Compound **4** also reacts instantaneously with the late-transition-metal anion, but it takes approximately 8 h to convert it to the dimer. During the intervening time, intermediates are formed and then disappear but the complexity of the spectra makes it impossible to state that a transient heterobimetallic species has been formed. The formation of the late-transition-metal dimer can be interpreted as reduction of **3** or **4** by the late-transition-metal anion. To determine if the failure to form stable bimetallics was due to the ease of reduction of our compounds, we measured the reduction potentials of **3** or **4** as well as those of Cp_2ZrX_2 (X = Cl, Br) via cyclic voltammetry.[23] Since the zirconocene dihalides (16-electron compounds) are not reduced by $MCp(CO)_2^-$ whereas **3** and **4** (14-electron complexes) are, we expected to find that our compounds would be the easier to reduce. This was not the case. Table VII shows the position of the first reduction wave for all four compounds along with the $E°_{red}$ for the zirconocene dihalides. Only the reductions of the zirconocene dihalides were reversible (our value for $E°_{red}$ compares favorably to the value of -2.3 V versus Ag/AgCl measured previously[24]). Nevertheless, since all of the compounds were measured under identical conditions, we can compare the position of the first reduction waves to see that compounds **3** and **4** are more difficult to reduce than the zirconocene dihalides. It therefore seems unlikely that Zr electron deficiency is responsible for the failure to form stable bimetallics unless allyl isomerization to an η^1 transition state renders it Zr electron deficient, inducing its reduction by the late-transition-metal anion. Another explanation for formation of the late-transition-metal dimer is homolytic cleavage of a transient Zr–M bond induced by steric bulk. That such bulk exists within the Cp*(η^3-$Me_3C_3H_2$)Zr moiety is demonstrated in the next set of reactions, in which we attempted to substitute both bromides in **3** and **4** with CH_2PPH_3 but instead isolated butadiene compounds.

$$\underset{\mathbf{3,\ 4}}{Cp^*(allyl)ZrBr_2} + 2LiCH_2PPh_2 \rightarrow \underset{\mathbf{5,\ 6}}{Cp^*Zr(butadiene)(CH_2PPh_2)} + 2LiBr + MePPh_2$$

allyl = 1,1,2-$Me_3C_3H_2$ (**3**), 1,2,3-$Me_3C_3H_2$ (**4**)

butadiene = 2,3-$Me_2C_4H_4$ (**5**), 1,2-$Me_2C_4H_4$ (**6**)

The butadiene ligand results from abstraction of an allyl terminal methyl proton by $PPh_2CH_2^-$ with subsequent formation of free $MePPh_2$, observed by NMR analysis. Evidently there is simply not enough room for coordination of a second CH_2PPh_2 ligand. This is in contrast to Cp_2ZrCl_2, which yields $Cp_2Zr(CH_2PPh_2)_2$.[20] The only other instance of $LiCH_2PPh_2$ abstracting a methyl proton was also attributed in large part to steric congestion.[11]

Isomers and Dynamic Behavior of Cp*(1,2,3-$Me_3C_3H_2$)$ZrBr_2$ (4). We reported earlier on the preparation and structure of **3** and **4** and on the dynamic behavior of **3**.[1] Both complexes contain an η^3-allyl ligand. Compound **3** was fluxional on the NMR time scale, undergoing rapid interconversion between enantiomers via an η^1 transition state ($\Delta G^‡$ = 51.5 kJ/mol). Measurement of the analogous barrier for **4** was not attempted due to its mirror symmetry. However, the ^{1}H NMR spectrum of **4** was measured on a low-field (80 MHz) instrument.[1] Reinvestigation of the ^{1}H NMR spectrum of **4** on a 300-MHz spectrometer has revealed the presence of a second isomer. The -20 °C ^{1}H NMR spectrum of **4** is shown in Figure 3. We have noted that syn-oriented methyls in Cp*(η^3-$Me_3C_3H_2$)MBr_2 complexes (M = Zr, Hf) appear around 2 ppm whereas anti-oriented methyls give rise to upfield signals between ~0.7 and 0.3 ppm.[1,25] The spectrum of the predominant isomer I is consistent with the solid-state structure in which the terminal allyl methyls are syn to the central methyl group. However, a second isomer is also observed (the ratio of I to II is 3.2:1 at 0.0 °C, yielding K_{eq} = [II]/[I] = 0.312; ΔG = 2.6 kJ/mol). The upfield doublet at δ 0.32 labeled Me_{II}^{ANTI} is a clear indication of an anti-oriented methyl. A complete variable-temperature data set measured in THF-d_8 from 0 to 100 °C leads to rapid (on the NMR time scale) exchange between isomers I and II. Such an exchange could be accomplished by an η^3–η^1 isomerization along with rotation

(23) Gassman, P. G.; Macomber, D. W.; Hershberger, J. W. *Organometallics* **1983**, *2*, 1470.

(24) Dessy, R. E.; King, R. B.; Waldrop, M. *J. Am. Chem. Soc.* **1966**, *88*, 5112.

(25) Hauger, B. E.; Vance, P. J.; Prins, T. J.; Wemple, M. E.; Kort, D. A.; Kelly, R. S.; Huffman, J. C.; Silver, M. E. Submitted for publication in *J. Organomet. Chem.*

(26) (a) Prout, K.; Cameron, T. S.; Forder, R. A.; Critchley, S. R.; Denton, B.; Rees, G. V. *Acta Crystallogr., Sect. B: Crystallogr. Cryst. Chem.* **1974**, *B30*, 2290. (b) Guggenberger, L. J. *Inorg. Chem.* **1973**, *12*, 232. (c) Melmed, K. M.; Coucouvanis, D. L.; Lippard, S. J. *Ibid.* **1973**, *12*, 232.

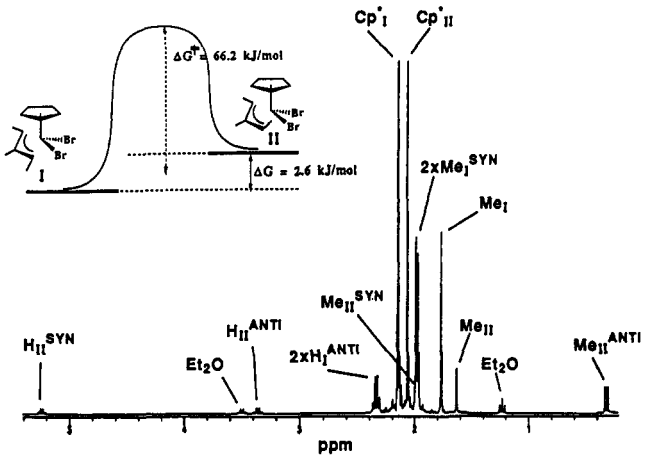

Figure 3. ^{1}H NMR spectrum (−20 °C) of Cp*(1,2,3-$Me_3C_3H_2$)-$ZrBr_2$ (4) in $CDCl_3$. (Cp* resonances are expanded off scale.) Subscripts I and II refer to isomers I and II shown above. Free energy values are derived from a variable-temperature ^{1}H NMR study.

about the C–C and Zr–C single bonds. The barriers for this process were measured to be $\Delta G^{\ddagger}$(I → II) = 70.0 ± 1.0 kJ/mol and $\Delta G^{\ddagger}$(II → I) = 66.5 ± 1.0 kJ/mol (estimated from the broadening of the Cp* signals observed at 15.0 °C relative to the −40.0 °C static spectrum using the slow-exchange approximation).[27] This is 15.0–18.5 kJ/mol higher than the barrier for **3**. Such an increase upon methyl substitution of both ends of the allyl ligand is expected.[6] Coalescence of the Cp* peaks occurred at 36.0 °C. Coalescence of the terminal methyl and CH signals into two broad peaks was also achieved at higher temperatures.

Molecular Structures for 1 and 6. Final atomic coordinates and equivalent isotropic thermal parameters for the non-hydrogen atoms of **1** and **6** are presented in Table II; bond distances and angles are given in Table VIII. Perspective views showing the molecular geometry and the atom-numbering schemes for **1** and **6** are presented in Figure 1 and Figure 2, respectively.

Molecular Structure for Cp*(C_3H_5)$ZrCl_2$ (1). In the orthorhombic unit cell for **1** each molecule lies on a crystallographic mirror plane passing through atoms C2, C3, C6, and Zr. The molecular structure of **1** is similar to that of a bent metallocene, however, the plane defined by the Zr and the two Cl atoms does not bisect the Ct(Cp*)–Zr–Ct(allyl) angle (Ct = centroid, the angle between the centroid-to-metal vector and its projection onto $ZrCl_2$ plane being 72.3 and 39.7° for the Cp* and allyl ligands, respectively). The Ct(Cp*)–Zr–Ct(allyl) angle of 112.0 (3)° is similar to the value of 118.4° found for Cp*(1,2,3-$Me_3C_3H_2$)$ZrBr_2$.[1] Crystallographic studies have shown that the corresponding Ct(Cp)–metal–Ct(Cp) angle in a bent metallocene can vary from 148° in Cp_2MoH_2 to 126° in Cp_2ZrI_2.[26]

As is often observed, all the Cp* methyl groups are displaced from the Cp* ring plane away from the Zr atom by approximately 0.1 Å. The normal to the Cp* plane is essentially colinear with the Zr–Ct(Cp*) vector (deviation is 2.7°). The small tilt of the Cp* ligand is directed away from the allyl ligand. A unique aspect of this structure is the prone geometry assumed by the η^3-allyl ligand relative to Cp*. All previous structures of Cp*(η^3-$Me_3C_3H_2$)MBr_2 complexes (M = Zr, Hf) have revealed a supine orientation for the allyl ligand.[1,25] In these cases the supine geometry minimized nonbonded repulsions by directing allyl methyls away from the Cp* ligand. Molecular mechanics minimization shows that even in the absence of allyl methyl substituents it is still the supine geometry that minimizes steric congestion (calculated difference in steric repulsion is 7.5 kJ/mol for **1**).[28]

Table VIII. Bond Distances (Å) and Angles (deg) for Cp*$Zr(C_3H_5)Cl_2$ (1) and Cp*Zr(1,2-dimethyl-1-3-butadiene)(CH_2PPh_2) (6)

atoms	dist	atoms	angle
	Compound 1		
Zr–Cl	2.4294 (16)	Cl–Zr–Cl′	96.12 (9)
Zr–C1	2.429 (7)	C1-C2-C1′	120.9 (10)
Zr–C2	2.504 (9)	C4–C3–C4′	107.9 (6)
Zr–C3	2.440 (7)	C4–C3–C6	125.9 (3)
Zr–C4	2.484 (5)	C3–C4–C5	108.6 (5)
Zr–C5	2.539 (5)	C3–C4–C7	126.2 (5)
C1–C2	1.376 (9)	C5–C4–C7	125.0 (5)
C3–C4	1.415 (7)	C4–C5–C5′	107.4 (3)
C3–C6	1.509 (11)	C4–C5–C8	126.4 (5)
C4–C5	1.418 (7)	C5′–C5–C8	125.9 (3)
C4–C7	1.500 (8)		
C5–C5′	1.442 (10)		
C5–C8	1.498 (8)		
	Compound 6		
Zr–P	2.6637 (21)	P–Zr–C7	40.85 (19)
Zr–Cl	2.351 (7)	Zr–P–C7	59.92 (24)
Zr–C2	2.486 (7)	Zr–P–C8	127.65 (22)
Zr–C3	2.447 (8)	Zr–P–C14	130.44 (23)
Zr–C4	2.304 (9)	C7–P–C8	112.4 (4)
Zr–C7	2.346 (8)	C7–P–C14	111.0 (3)
Zr–C20	2.506 (7)	C8–P–C14	101.5 (3)
Zr–C21	2.518 (7)	C2–C1–C5	120.7 (7)
Zr–C22	2.530 (8)	C1–C2–C3	120.2 (7)
Zr–C23	2.514 (7)	C1–C2–C6	119.6 (7)
Zr–C24	2.520 (7)	C3–C2–C6	120.0 (7)
P–C7	1.774 (8)	C2–C3–C4	122.8 (8)
P–C8	1.835 (7)	Zr–C7–P	79.2 (3)
P–C14	1.840 (7)	P–C8–C9	123.1 (6)
C1–C2	1.434 (11)	P–C8–C13	117.9 (6)
C1–C5	1.523 (11)	C9–C8–C13	119.0 (7)
C2–C3	1.396 (11)	C8–C9–C10	119.6 (7)
C2–C6	1.509 (11)	C9–C10–C11	121.0 (8)
C3–C4	1.434 (12)	C10–C11–C12	119.5 (8)
C8–C9	1.365 (10)	C11–C12–C13	119.5 (8)
C8–C13	1.390 (11)	C8–C13–C12	121.4 (8)
C9–C10	1.394 (11)	P–C14–C15	118.4 (5)
C10–C11	1.377 (11)	P–C14–C19	121.8 (6)
C11–C12	1.369 (12)	C15–C14–C19	119.7 (7)
C12–C13	1.377 (12)	C14–C15–C16	119.5 (8)
C14–C15	1.392 (11)	C15–C16–C17	120.9 (8)
C14–C19	1.385 (10)	C16–C17–C18	119.8 (8)
C15–C16	1.386 (11)	C17–C18–C19	120.4 (7)
C16–C17	1.367 (12)	C14–C19–C18	119.7 (7)
C17–C18	1.378 (11)	C21–C20–C24	108.3 (6)
C18–C19	1.388 (10)	C21–C20–C25	126.0 (7)
C20–C21	1.438 (10)	C24–C20–C25	125.3 (7)
C20–C24	1.422 (11)	C20–C21–C22	107.4 (6)
C20–C25	1.508 (11)	C20–C21–C26	126.5 (7)
C21–C22	1.413 (10)	C22–C21–C26	126.0 (7)
C21–C26	1.492 (11)	C21–C22–C23	108.4 (6)
C22–C23	1.433 (11)	C21–C22–C27	124.9 (7)
C22–C27	1.498 (11)	C23–C22–C27	126.3 (7)
C23–C24	1.420 (10)	C22–C23–C24	108.0 (7)
C23–C28	1.487 (12)	C22–C23–C28	126.3 (7)
C24–C29	1.489 (11)	C24–C23–C28	125.4 (7)
		C20–C24–C29	127.0 (7)
		C23–C24–C20	107.9 (7)
		C23–C24–C29	125.0 (7)

(27) (a) Emsley, J. W.; Freeney, J.; Sutcliffe, L. H. *High Resolution Nuclear Magnetic Resonance Spectroscopy*; Pergamon Press: Oxford, U.K., 1965, Vol. 1, pp 481. (b) Anet, F. A. L. *J. Am. Chem. Soc.* **1964**, *86*, 458.

(28) Modeling calculations were carried out by using an extended version of Allinger's MM2 force field, which includes transition metals. The programs were obtained from Serena Software Inc., P.O. Box 3076, Bloomington, IN 47402.

Adoption of the sterically less favorable prone orientation might be due to either electronic or crystal-packing forces. The allyl ligand tilts away from Cp*, as is observed elsewhere,[1,25] the angle between the normal to the allyl ligand plane and the Zr–Ct(allyl) vector being 33.1°. This results in a slightly longer bond from Zr to the interior allyl carbon atom than it does to the terminal ones [Zr–C2, 2.504 (9) Å; Zr–Cl, 2.429 (7) Å].

Molecular Structure for Cp*(1,2-Me₂C₄H₄)(CH₂PPh₂)Zr (6). In the triclinic unit cell for **6** there are two molecules occupying general positions. The molecular structure of **6** is also similar to that of a bent metallocene, with a Ct(Cp*)–Zr–Ct(butadiene) angle of 139.8 (4)°. All the Cp* methyl groups are displaced out of the Cp* plane away from the Zr atom by approximately 0.1 Å. The normal to the Cp* plane is essentially colinear with the Zr–Ct(Cp*) vector (deviation is 0.4°). The butadiene ligand is η^4-bound and is in a supine orientation with respect to Cp*. The butadiene also tilts toward Cp* and away from the CH_2PPh_2 ligands, the angle between the normal to the butadiene ligand plane and the Zr–Ct(butadiene) vector being 27.4°. This tilt is reflected in slightly longer Zr–carbon distances to the inner carbon atoms [Zr–C2, 2.486 (7) Å; Zr–C3, 2.447 (8) Å] than to the outer carbon atoms [Zr–Cl, 2.351 (7) Å; Zr–C4, 2.304 (9) Å]. Such a tilt slightly distorts the η^4-butadiene toward a σ^2-π mode, resulting in a slightly shorter C2–C3 bond (1.396 Å) relative to the C1–C2 and C3–C4 bonds (both 1.434 Å). An unusual feature of this structure involves the η^2-bonding of the CH_2PPh_2 ligand. Previous structural determinations of $Cp_2Zr(Cl)CH_2PPh_2$,[29] $Cp_2Zr(CH_2PPh_2)_2$,[29] and $Cp^*_2Zr(Cl)CH_2PPh_2$[30] revealed an η^1-binding mode through the CH_2 group. Indeed, it has been noted that all group IV d^0 complexes of CH_2PPh_2 are exclusively η^1.[29] The preference for η^1-binding to early-transition metals has been blamed on unfavorable steric interactions involving the phenyl groups, since extended huckel calculations show the η^2 mode to be favored for the hypothetical $Cp_2Zr(Cl)CH_2PH_2$.[31] Interestingly, there is ESR evidence for bidentate coordination in the reduced Zr(III) species $(C_5H_4$-*t*-Bu$)Zr(CH_2PPh_2)_2$ and $(C_5H_4$-*t*-Bu$)ZrH(CH_2PPh_2)$.[32] Compound **6** therefore represents the first structurally characterized example of a Zr complex possessing an η^2-CH_2PPh_2 ligand. The Zr–C bond length [Zr–C7, 2.346 (8) Å] is longer than observed for η^1-CH_2PPh_2 complexes of Zr in which the P atom does not bridge to another metal [2.281 Å, $Cp_2Zr(CH_2PPh_2)Cl$; 2.284 and 2.340 Å, $Cp_2Zr(CH_2PPh_2)_2$].[29] However, the Zr–P bond (Zr–P, 2.6637 Å) is within the range of previously reported Zr–P bond distances (2.607–2.839 Å).[33-38] The resulting three-membered Zr–C–P ring is strained, possessing Zr–C–P, C–P–Zr, and P–Zr–C angles of 79.2 (3), 59.9 (2), and 40.8 (2)°, respectively. It should be noted that the related phosphine ligand in $Cp_2ZrCl[CH_2P(SiMe_3)_2]$ is also η^2-bound with Zr–C and Zr–P distances of 2.607 and 2.606 Å, respectively.[38] Finally, there are a number of repulsive contacts within the molecule (C1–C25, 0.337 Å; C2–C7, 0.321 Å; C4–C29, 0.353 Å; C5–C25, 0.342 Å; C6–C7, 0.421 Å; C7–C27, 0.612 Å; values represent the amount that the nonbonded distances are within the sum of the appropriate van der Waals radii[39]).

Dynamic Behavior of Cp*(2,3-Me₂C₄H₄)(CH₂PPh₂)Zr (5). The X-ray structure of **6** revealed an η^2-CH_2PPh_2 ligand bound to Zr at the C and P atoms. Suitable crystals for structure determination could not be obtained for **5**. However, it is reasonable to postulate that **5** has a structure similar to that of **6**. The low-temperature (−104 °C) ^1H NMR spectrum is consistent with this, yielding separate signals for the P–CH_2 protons and for each proton and methyl group in the butadiene ligand. However, upon warming to room temperature, there is a dynamic process that exchanges inequivalent butadiene exo, endo, methyl, and P–CH_2 signals with each other. The $\Delta G^\ddagger$ for this process, measured from the coalescence of the P–CH_2 (−76 °C), butadiene endo (−76 °C), and methyl (−88 °C) signals was 38.9 ± 1 kJ/mol. No known dynamic processes involving the butadiene ligand could produce the observed NMR behavior.[33,40-42] A mechanism that does involves Zr–P bond rupture followed by rotation about the Zr–CH_2 bond and subsequent reattachment of the P to yield the enantiomer. It should be noted that while the barrier for this process seems low considering that the Zr–P bond in related compound **6** is among the shortest yet observed, the structure of **6** also revealed a highly strained Zr–C–P ring.

Conclusions

The low yields of $Cp^*(C_3H_5)ZrCl_2$ and $Cp^*(C_3H_5)ZrBr_2$ complexes are apparently due to unfavorable kinetics which favor formation of $Cp^*Zr(allyl)_3$ compounds. However, if the allyl ligand is terminally methylated, the yields are substantially higher. This is most likely due to the fact that tris(allyl) complexes of terminally methylated allyl ligands can decompose to stable butadiene intermediates, which can then go on to ligand exchange with unreacted Cp^*ZrCl_3 and yield the desired product. The reactivity of $Cp^*(\eta^3$-$Me_3C_3H_2)ZrBr_2$ compounds is drastically different from that of the closely related zirconocene dihalides. While the bromides are easily substituted, products similar to those isolated from zirconocene dihalides are not obtained. Instead, compounds are isolated which seem to indicate that Cp*(allyl)Zr is a more crowded moiety than Cp_2Zr, resulting in the inability to form stable heterobimetallics upon substituting $[MCp(CO)_2]^-$ (M = Fe, Ru) for one bromide or $Cp^*(methylallyl)Zr(CH_2PPh_2)_2$ complexes upon substitution of $PPh_2CH_2^-$ for both bromides. However, the latter attempt yielded the first structurally characterized example of an early-transition-metal η^2-bound to a CH_2PPh_2 ligand. Finally, the inability to form stable heterobimetallics with $[MCp(CO)_2]^-$ may be

(29) Schore, N. E.; Young, S. J.; Olmstead, M. M.; Hofmann, P. *Organometallics* **1983**, *2*, 1769.
(30) Young, S. J.; Olmstead, M. M.; Knudsen, M. J.; Schore, N. E. *Organometallics* **1985**, *4*, 1432.
(31) Hofmann, P.; Stauffert, P.; Schore, N. E. *Chem. Ber.* **1982**, *115*, 2153.
(32) Choukroun, R.; Gervais, D.; Rifai, C. E. *J. Organomet. Chem.* **1989**, *368*, C11.
(33) Fryzuk, M. D.; Haddad, T. S.; Rettig, S. J. *Organometallics* **1989**, *8*, 1723.
(34) Green, M. L.; Mountford, P.; Walker, N. M. *J. Chem. Soc., Chem. Commun.* **1989**, 908.
(35) Stahl, L.; Hutchinson, J. P.; Wilson, D. R.; Ernst, R. D. *J. Am. Chem. Soc.* **1985**, *107*, 5016.
(36) Wengrovius, J. H.; Schrock, R. R.; Day, C. S. *Inorg. Chem.* **1981**, *20*, 1844.
(37) Wieistra, Y.; Meetsma, A.; Gambarotta, S. *Organometallics* **1989**, *8*, 258.
(38) Karsch, H. H.; Deubelly, B.; Hofmann, J.; Pieper, U.; Muller, G. *J. Am. Chem. Soc.* **1988**, *110*, 3654.
(39) Pauling, L. *The Nature of the Chemical Bond*, 3rd ed; Cornell University: Ithaca, NY, 1960; p 260. Pauling gives the van der Waals radius of a methyl group and an aromatic CH as 2.0 and 1.7 Å, respectively. A lower limit of 1.45 Å, the covalent radius of Zr, is taken for the van der Waals radius, which is unknown.
(40) Erker, G.; Engel, K.; Korek, U.; Czisch, P.; Berke, H.; Caubere, P.; Vanderesse, R. *Organometallics* **1985**, *4*, 1531.
(41) Spielvogel, B. F.; Das, M. K.; McPhail, A. T.; Onan, K. D.; Hall, I. H. *J. Am. Chem. Soc.* **1980**, *102*, 6344.
(42) Erker, G.; Kruger, C.; Muller, G. *Adv. Organomet. Chem.* **1985**, *24*, 1.

due to allyl η^3 to η^1 isomerization.

Acknowledgment is made to the National Science Foundation RUI program (Grant No. CHE-8800845), the National Science Foundation REU program (Grant No. CHE-8804803), and to the Camille and Henry Dreyfus Foundation Teacher-Scholar Program.

Supplementary Material Available: Tables of thermal parameters and hydrogen atom coordinates (Tables III and IV) (2 pages); listings of observed and calculated structure factors (Tables V and VI) (11 pages). Ordering information is given on any current masthead page.

Catalytic Dehydrogenative Coupling of Secondary Silanes with Cp_2MCl_2/nBuLi

Joyce Y. Corey,* Xiao-Hong Zhu, Thomas C. Bedard, and Lura D. Lange

Department of Chemistry, University of Missouri—St. Louis, St. Louis, Missouri 63121

Received August 22, 1990

The catalytic dehydrogenative coupling of secondary silanes has been achieved with the combination of Cp_2ZrCl_2 and 2 equiv of nBuLi in toluene at 90 °C. The products produced from $PhMeSiH_2$ contain disilane through pentasilanes after 2 days, and longer time periods produce oligomeric mixtures up to the octamer. Disilane through tetrasilane have been isolated as distillable, air-stable liquids and are produced as mixtures of stereoisomers. The distribution of oligomers has been determined under various conditions of temperature, time, solvent, and Si/Zr and Zr/Li ratios as well as with a combination of Cp_2ZrCl_2 with Grignard reagents. Disilane is formed from Ph_2SiH_2 even at 110 °C, although silafluorene condenses rapidly even at room temperature to a mixture of oligomers. The combination of Cp_2TiCl_2/nBuLi with $PhMeSiH_2$ provides oligomers from disilane through hexasilane, whereas Cp_2HfCl_2 produces disilane and trisilane. A possible mechanism for the coupling reaction is presented.

Introduction

The chemistry of short silicon chains is an undeveloped area in group XIV chemistry. The general method utilized to form silicon–silicon bonds is a Wurtz-type coupling reaction of halosilanes (usually chlorosilanes).[1] The products from this reaction are cyclopolysilanes or linear polysilanes depending on the reaction conditions employed. Although halogen-terminated oligomers are probable intermediates in the condensation reaction, these are rarely reported.[2] Thus, oligomers are usually prepared either by multistep routes that require the formation of a cyclopolysilane followed by ring opening or by some variant of a Wurtz-type coupling reaction of a dihalosilane in the presence of a monohalosilane as a chain terminator.[1c]

Harrod and co-workers have shown that it is possible to generate silicon oligomers from primary silanes in the presence of metallocene complexes. The best catalysts for the dehydrogenative coupling are those derived from Cp_2MR_2 (M = Ti, Zr; R = Me).[4] The condensation of $PhSiH_3$ produced the linear oligomers $H(PhSiH)_xH$ with an average degree of polymerization of 10 from Cp_2TiMe_2[5] and 20 from Cp_2ZrMe_2.[6] However, $BuSiH_3$ is converted to both linear and cyclic products with Dp values ranging between 2 and 8 with Cp_2ZrMe_2.[7]

Table I. Diastereomers of $H(PhMeSi)_xH$

	no. of stereoisomers		no. of Me resonances		no. of resonances
x	meso forms	d,l pairs	^1H	$^{13}C^a$	$^{29}Si^b$
2	1	1	4[c]	2	2
3	2	1	11[d]	7	7
4	2	4	24[e]	16	16

[a] Decoupled. [b] If observable. [c] Two doublets. [d] Four doublets and three singlets. A statistical mixture would contain 10 resonances of intensity 1 and the remaining resonance of intensity 2. [e] Eight doublets (four of intensity 1 and four of intensity 2) and eight singlets (four of intensity 1 and four of intensity 2).

The conversion of secondary silanes to oligomers has been much less successful. Dimerization of $PhMeSiH_2$ occurs with catalytic quantities of Cp_2ZrMe_2[8] and Cp_2TiMe_2[9] but only in the presence of an olefin in the latter case. Under rigorous conditions (110 °C) Cp_2TiPh_2 converts $PhMeSiH_2$ to disilanes and trisilanes and addition of an olefin improves conversion of the starting material and favors the trisilane product.[10]

There are disadvantages in the use of Cp_2MR_2 catalysts, which include the required synthesis from a metallocene dichloride and the fact that Cp_2ZrMe_2 undergos slow decomposition at room temperature. A more direct approach to catalysis by the metallocene complexes of the titanium triad would be generation in situ of an active species directly from the metallocene dichloride. Described in this report is the combination of commercially available Cp_2MCl_2 and nBuLi, which produces a catalyst capable of generating oligomers with more than three silicon atoms from secondary silanes, in contrast to the results reported for Cp_2MR_2.

(1) (a) West, R. In *The Chemistry of Organic Silicon Compounds*; Patai, S., Rappoport, Z., Eds. Wiley: New York, 1989; Vol. II, Chapter 19. (b) Miller, R. D.; Michl, J. *Chem. Rev.* **1989**, *89*, 1359. (c) Hengge, E. *Phosphorus Sulfur* **1986**, *28*, 43.

(2) Two examples are a 1,2-dichlorodisilane from the condensation of $tBuPhSiCl_2$ with a deficiency of lithium[3a] and a 1,3-dichlorotrisilane produced from $(c\text{-}C_6H_{11})_2SiCl_2$ with Li/Naph.[3b].

(3) (a) Matsumoto, H.; Sakamoto, A.; Minemura, M.; Sugaya, K.; Nagai, Y. *Bull. Chem. Soc. Jpn.* **1986**, *59*, 3314. (b) Weidenbruch, M. Presented at the VIIth International Organosilicon Symposium, St. Louis, 1987; Abstract B26.

(4) Aitken, C.; Barry, J.-P.; Gauvin, F.; Harrod, J. F.; Malek, A.; Rosseau, D. *Organometallics* **1989**, *8*, 1732 and references therein.

(5) Aitken, C.; Harrod, J. F.; Gill, U. S. *Can. J. Chem.* **1987**, *65*, 1804.

(6) Harrod, J. F. *Polym. Prepr. (Am. Chem. Soc., Div. Polym. Chem.)* **1987**, *28*, 403.

(7) Campbell, W. H.; Hilty, T. K.; Yurga, L. *Organometallics* **1989**, *8*, 2615.

(8) Aitken, C.; Harrod, J. F.; Samuel, E. *Can. J. Chem.* **1986**, *64*, 1677.

(9) Harrod, J. F.; Yun, S. S. *Organometallics* **1987**, *6*, 1381.

(10) Nakano, T.; Nakamura, H.; Nagai, Y. *Chem. Lett.* **1989**, 83.

0276-7333/91/2310-0924$02.50/0